

Non-Linearities of the BOLD Response in the Human Brain

By Jeffrey C. McCullough

Abstract

In this study, event-related functional magnetic resonance imaging (fMRI) studies were performed on healthy volunteers at 7 Tesla (T), the highest field strength currently available for human studies. This study assessed the linearity of the hemodynamic response to short-duration stimuli of 0.25s, 0.5s, 1.0s, and 2.0s. This study expected clearer resolution at 7T.

Results showed that the hemodynamic response at short duration stimulus exhibited non-linear characteristics. Analysis of response location showed a clustered dispersion to the observed non-linearity. Noteworthy discrepancies were found between the non-linear aspects of the hemodynamic responses in this study when compared to a previous study done at 4T. Unique to this study was the initial creation of a linearity index map, showing the spatial clustering of the non-linearity.

Introduction

In previous neuroimaging studies of the human brain, it has been suggested that hemodynamic response to long-duration stimuli (visual or auditory) shows a linear relationship. The purpose of this study was to determine the linearity of the hemodynamic response to short duration stimuli less than two seconds. It is important to determine whether the relationship between stimulus duration and BOLD response is different for different durations so that the physiologic significance of the response can be accurately determined. The hypotheses of this study were:

- 1) There would be a non-linear relationship between stimulus duration of less than two seconds in the hemodynamic response using event-related BOLD functional magnetic resonance imaging (fMRI) at high magnetic field strength of 7 Tesla (T).
- 2) The higher field strength would give sufficiently clear resolution to show that the non-linearity is spatially clustered in the human brain.

Background

The technique of fMRI is used to image brain activity at video rates (30 milliseconds/image) while the brain is functioning. Since active brain cells use oxygen, the activity of the cells can be detected and seen as 'activated' against a background of less active cells. Changing levels of deoxyhemoglobin are sufficient to cause measurable changes in the blood-oxygen level in the visual cortex (1). Mapping regions of the brain that control motor functions is possible because of these changes.

Most fMRI studies assume a linear relationship to model stimulus duration versus corresponding BOLD response (2), but Vazquez and Noll in 1998 suggested that at short duration stimuli the relationship might be non-linear (3). Therefore knowing the true nature of the relationship between stimulus duration and BOLD response is crucial to response modeling.

Vazquez and Noll reported that the hemodynamic response to stimuli of less than four seconds at 1.5T was non-linear; therefore short duration stimuli could not be used to predict responses to long-duration stimuli (3). In a 2000 study, Pfeuffer (4) showed that non-linear relationships existed for stimulus duration (SD) less than two seconds at 4T. Using short-duration stimuli, he

showed that the BOLD response exhibited strong non-linear characteristics in both amplitude and width. Yacoub *et. al.* (5) showed that the sensitivity and spatial specificity are improved at 7T. This suggests that ultrahigh field magnetic resonance systems are advantageous for functional mapping in humans. The study reported in this paper dealt with the non-linear aspects of the hemodynamic response done at 7T in order to improve spatial specificity. Since non-linearity in the BOLD response has been reported using 1.5 and 4T instruments, and 7T instruments provide more sensitive and accurate readings, this study was designed to use the most sensitive techniques presently available to establish whether the BOLD response to short duration stimuli in non-linear.

Methods:

Data Acquisition

Healthy volunteers were subjects in this study. This author assisted Professor Pfeuffer in carrying out scans using event-related fMRI with a 7T Magnex magnet/Varian INOVA capsule, the largest magnet for human studies in the world. Heart rate and respiration of volunteers were monitored to correct for movement artifacts from heartbeats and breathing. Visual stimuli were presented to the volunteers using light-emitting diode goggles with a flashing checkerboard pattern. Images were obtained to identify the slice of interest. Event-related studies were performed at a 256 x 40 matrix size, 4.8-cm field of view, and 1.2 x 1.2 x 3.0 mm³ voxel (volumetric pixel) size. In the event-related stimulus series, repetition time was 0.125s; SD was 0.25s, 0.5s, 1s, & 2s; inter-stimulus interval was 18s with 16 trials per scan.

Data Processing

Each scan consisted of multiple trials, which were averaged to increase signal to noise ratio. Averaging over the total series was required to assess interseries movement between trials. When movement was detected, the series was discarded. The data were analyzed using *Stimulate*, a fMRI data analysis statistical software package developed at the University of Minnesota (6). Realignment, spatial normalization, spatial smoothing, voxel by voxel and statistical analysis were required for data analysis (7). Parametric maps, or 'activation maps', were calculated from the data and overlaid onto anatomic MR images for direct spatial comparison.

The generation of 'activation maps' to identify areas of brain activity was the primary data processing step. To test the activation intensity significance, it was necessary to assess the probability that the maximum value in the map was greater than a given threshold under the null hypothesis (8). The neural responses elicited by a given task gave rise to hemodynamic effects, which were sampled at discrete intervals by the scanner. In a student t-test, the fMRI signal for a given voxel was split into two sections, the baseline part and the activated part. The difference in means of the two parts divided by a measure of the standard deviation for the two parts was modeled by the student t-distribution and t-measure and/or probability measure for the two parts being equal was derived. This identified voxels that passed a predetermined confidence level, then calculated a percentage change from baseline value and presented it as a color image on an activation map (6). The data were then realigned to a reference image, spatially normalized and smoothed (9). Plots of the intensity time course were displayed for those voxels in a region of interest (ROI).

A cross-correlation method for parameter map generation was used to measure the temporal cross correlation between the paradigm and the measured data, using a Gaussian model for correlation against the intensity time course of each voxel in the functional image (10). Cross-correlation values for voxels were used to plot activation maps showing correlation value or percent intensity change in areas with correlation coefficients over a specified threshold. To obtain an equal number of activated voxels across series, a varying threshold was employed.

"Masks", generated through a series of specified algorithms and processing operations, were directly superimposed using a color overlay onto anatomical images. Cross correlation maps of the 400 most highly activated voxels were calculated on a voxel by voxel basis against a Gaussian function, then integrated. The voxel onset time was used to categorize voxels as $t_{on} < 2s$, $2s < t_{on} < 3s$, or $t_{on} > 3s$. The relative time versus percent relative BOLD change was plotted for each time classification.

Results

Figure 1 shows voxel correlation coefficients overlaid onto an image showing gray, white, and surrounding matter in the brain, where yellow is most strongly correlated with a Gaussian function and red is less strongly correlated.

Figure 1: Visual Cortex Activation

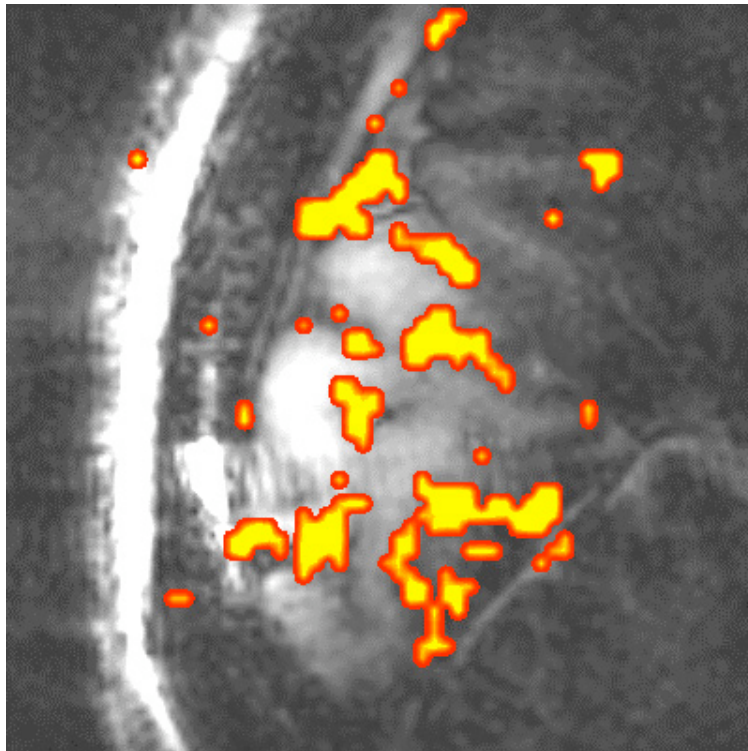
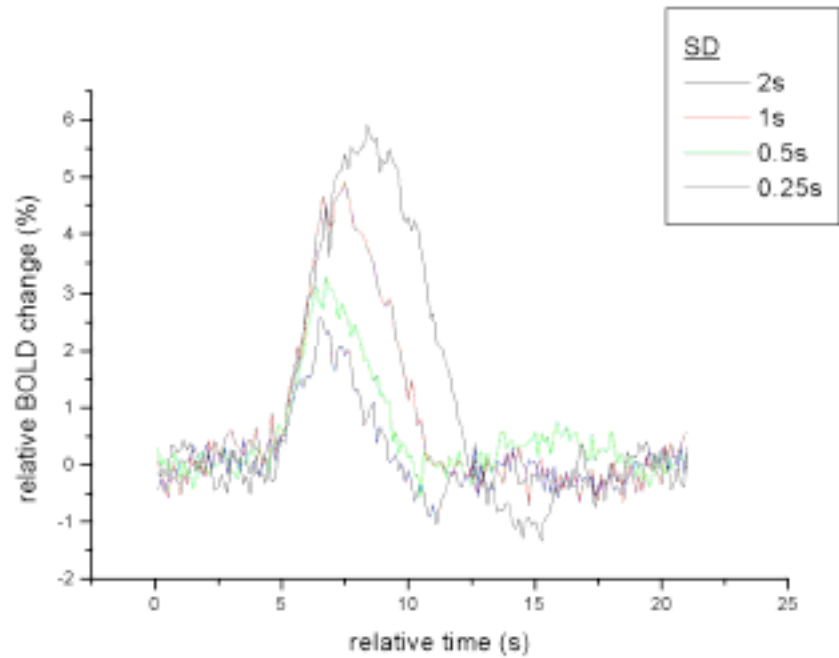


Figure 2 shows relative time versus relative BOLD percent change plotted at different SD, which was then smoothed resulting in the graph seen in Figure 3.

Figure 2: Averaged Time Course Relative BOLD Percent Change



Both figures show a sharp initial increase in BOLD levels, with a derivative consistent across all SD series. After reaching a peak, the BOLD levels decreased with a smaller derivative than the rise. After a return to baseline levels, an undershoot occurs, dipping the BOLD levels below their initial values, then returning to original levels.

Figure 3: FFT Filtered Averaged Time Course Relative BOLD Percent Change

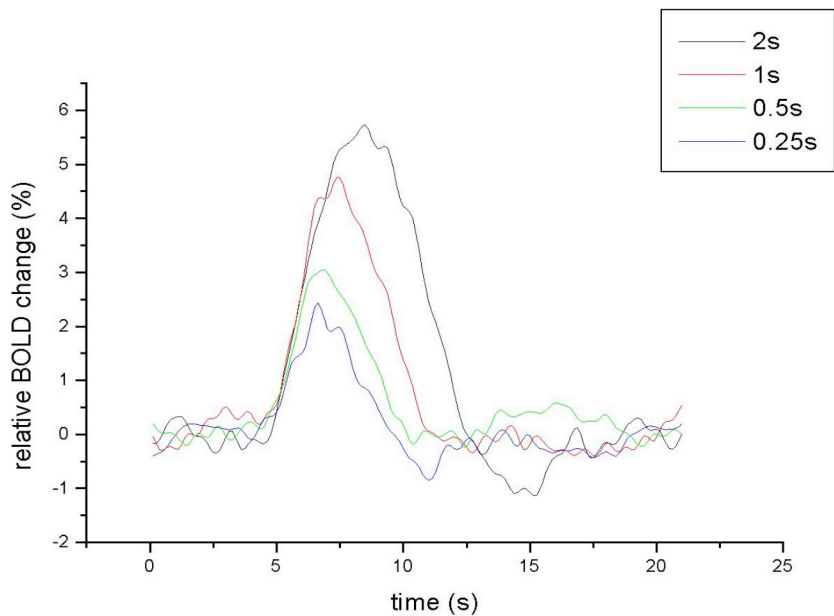


Figure 4 shows a plot of voxel linearity coefficients where red shows coefficients that are less than 0.8, orange are between 0.8 and 0.9, and yellow are greater than 0.9. The figure shows a clustered non-linearity, since individual colors are not randomly dispersed.

Figure 4: Voxelwise Linearity Index Map ($0.8 < LI < 0.9$)

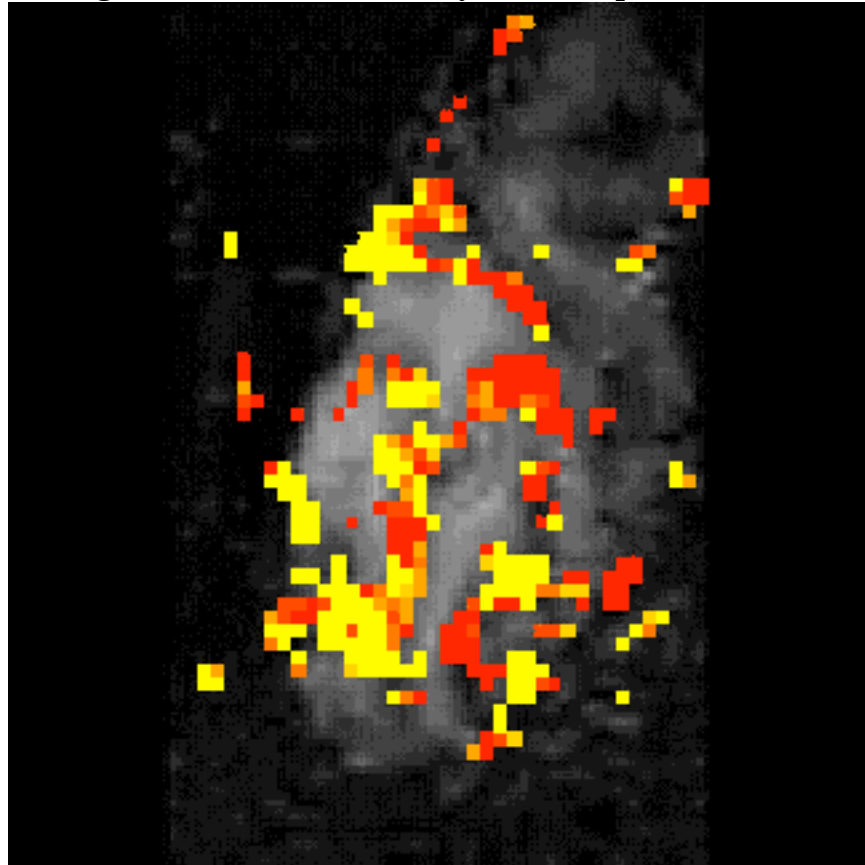


Figure 5 shows a scatter plot of values of normalized response integrals to stimuli of durations 0.1s, 0.2s, 0.4s, 0.8s, and 1.6s, plotted from data collected at 4T by Pfeuffer in 2000. An assumed linear model was used to calculate percent deviation, which is shown in Figure 6. Data obtained at 4T (4) were compared to data obtained at 7T. A linear pattern starts at the origin and continues to rise with constant slope. The line of best fit to the data shows a y-intercept at 0.3. From this data modeling, percent deviation from the predicted intensity was calculated as seen in Figure 6. A linear response to the stimuli would have shown a constant deviation of 0% while these data show more than a 400% deviation at 0.25s SD.

Figure 5: 4T Integrated Non-Linearity

Figure 6: 4T Intensity Non- Linearity

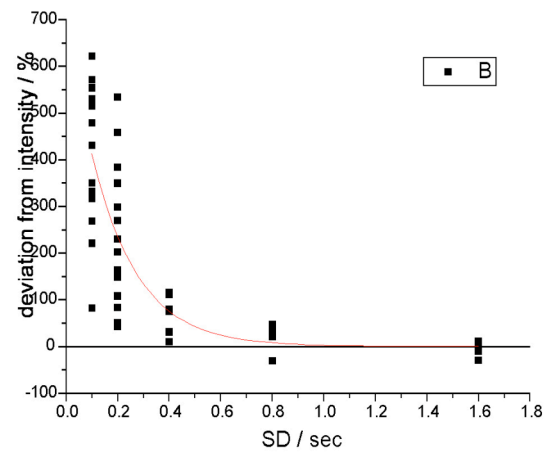
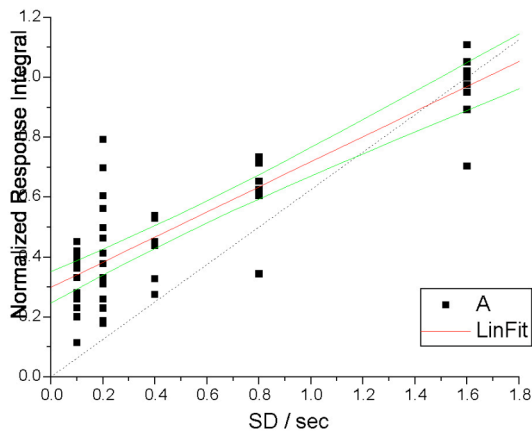
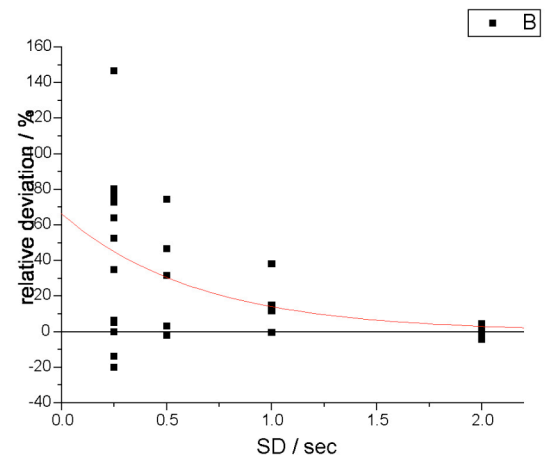
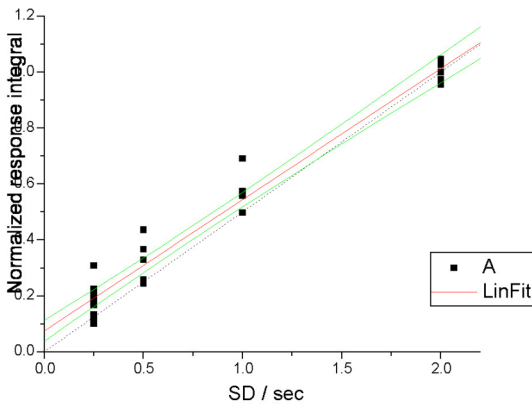


Figure 7 shows integral-value scatter plots from 7T data. The y-intercept of the 7T data line of best fit is less than 0.1 as opposed to 0.3 at 4T. Figure 9 shows percent deviation from intensity, which was less than 70% at 0.25s SD, whereas it was more than 400% at 4T.

Figure 7: 7T Integrated Non-Linearity

Figure 8: 7T Intensity Non-Linearity



Discussion

The hemodynamic response to short duration visual stimuli was shown to be non-linear: the 95%-confidence bands bars did not extend to the line of linearity at both 4T and 7T, as seen in Figures 6 and 8. The SD increased eight times across series, whereas the BOLD response increased only 4.3 fold, and the width of the response functions increased only 1.8 fold. This shows a significant deviation from linearity.

The voxels were compared across tissues and series to determine ‘sites’ of non-linearity. As seen in Figure 5, a linearity-index map was created, which shows a spatially clustered non-linearity. Through visual inspection, the voxel-specific analysis of gray, white, and surrounding matter showed the non-linearity of the hemodynamic BOLD response to be strongly associated with the

gray matter of the brain and less strongly associated with the white and surrounding matter of the brain.

Although the specific paradigms (voxel size, SD, repetition time, number of trials, etc.) of the 4T and 7T studies were not the same, logical conclusions can be made regarding discrepancies between the data. The y-intercept of the best-fit normalized response integral as seen in Figures 5 and 7 decreased from 0.3 to less than 0.1. The 95%-confidence bands on the 4T data extend down to approximately 0.25, whereas the 7T 95%-confidence bands reach only to 0.12. Thus, the difference in the linear-fit models is statistically significant. Percent deviation of the response data from linear was also statistically significant between 4T and 7T; the 4T data show a deviation of greater than 400%, i.e. the linear model prediction based on a 1.6s SD response to a 0.1s SD response was off by over 400%. The 7T data show only a 70% deviation when 2s SD responses are used to model 0.25s SD responses, showing a noteworthy difference.

Conclusion

At short duration stimuli, the BOLD signal exhibited non-linear characteristics. Voxel by voxel analysis showed a clustered dispersion to the observed non-linearity. Studies done at 4T and 7T imply a correlation between magnetic field strength and the non-linearity of the BOLD response to short duration visual stimuli, but to scientifically conclude this, further study is necessary.

Acknowledgements

I acknowledge the CMRR staff, Dr. Ugurbil and Dr. Hu for their guidance and leadership of the Hu group, Dr. Peuffer for guidance in background research, project design and implementation, data analysis, and sharing data from a previous study, Mrs. Fruen for the preparation of the paper, and Dr. McCullough for project arrangements and paper preparation.

Appendix B: Statistical Methods

The normal distribution, reasonably approximated for large sample size by the Gaussian distribution (used in this study to model the hemodynamic response to visual stimuli), describes the distribution of random observations for many experiments as well as describing the distributions obtained when the parameters of most other probability distributions are estimated

$$P_g = \frac{1}{\sigma_x \sqrt{2\pi}} * e^{-\frac{(x-X)^2}{2\sigma_x^2}} \quad (11).$$

More specifically the Gaussian distribution is an approximation to the binomial distribution for the special limiting case where the number of possible different observations becomes infinitely large and the probability of success for each is infinitely large. In a Gaussian distribution, the points X plus or minus the standard deviation are the two points of inflection. The distribution is reasonable, has a fairly simple analytic form, and it is accepted by convention and experimentation to be the most likely distribution for most experiments. Additionally, the most probable estimate of the mean from a random sample of observations is the average of those observations. It is a continuous function describing the probability of obtaining the value x in a random observation from a parent distribution with parameters corresponding to the mean and standard deviation. A given interval must be defined such that the probability that the value of a random observation will fall within an interval around x (12). The width of the curve is

dependent upon the standard deviation and symmetric about the mean. Regionally specific effects are framed in terms of differences among parameter estimates (an activation effect) and are specified using linear compounds or contrasts (13). The significance of each contrast is assessed with a statistic, with a student's t distribution under the null hypothesis.

Works Cited

1. Just MA, Carpenter PA, Keller TA, Emery L, Zajac H, Thulborn KR. Interdependence of Nonoverlapping Cortical Systems in Dual Cognitive Tasks. *Neuroimage* 14(2): 417-26. 2001.
2. Glover GH. Deconvolution of Impulse Response in Event-Related BOLD fMRI. *Neuroimage* 9(4): 416-429. 1999.
3. Vazquez, AL and Noll, DC. Nonlinear Aspects of the BOLD Response in Functional MRI. *Neuroimage* 7: 108-118. 1998.
4. Peuffer J, van de Moortele, PF, Adriany G, Auffermann WF, Ugurbil K, Hu X. Non-Linearities in Event-Related BOLD fMRI Using Very Short Stimulus Duration- A Study with High Temporal Resolution and Voxel Specific Analysis. *Proc. Intl. Soc. Mag. Res. Med* 8. 2000.
5. Yacoub E, Shmuel A, Pfeuffer J, van de Moortele, PF, Adriany G, Anderson P, Vaughan JT, Merkle H, Ugurbil K, Hu X. Imaging Brain Function in Humans at 7 Tesla. *Magn Res Med* 45(4): 588-594. 2001.
6. Strupp JP. 1996. "Stimulate: A GUI based fMRI Analysis Software Package." *Neuroimage*, 3(3): s306.
7. Friston KJ *et al.* Nonlinear Event-Related Responses in fMRI. *Mag. Reson. Med.* 39(1): 41-52. 1998.
8. Poline JB, Holmes A, Worsley JK, and Friston KJ. Statistical Inference and the Theory of Gaussian Fields. *SPM Short Course Notes*. Wellcome Department of Cognitive Neurology. 1997.
9. Howseman A, Josephs O, Rees G, and Friston KJ. *Special Issues in Functional Magnetic Resonance Imaging*. *SPM Short Course Notes*. Wellcome Department of Cognitive Neurology. 1997.
10. Press WH, Teuolsky SA, Vetterling WT, Flannery BP. *Numerical Recipes in C: The Art of Scientific Computing*. Cambridge University Press: Cambridge. 1992.
11. Taylor JR. *An Introduction to Error Analysis: The Study of Uncertainties in Physical Measurements*. University Science Books, Sausalito. 208-221. 1997.
12. Bevington PR and Robinson DK. *Data Reduction and Error Analysis for the Physical Sciences*. McGraw Hill, Boston. 81-93. 1992.
13. Kleinschmidt A, Requardt M, Merboldt KD, and Frahm J. On the Use of Temporal Correlation for Magnetic Resonance Mapping of Functional Brain Activation: Individualized Thresholds and Spatial Response Delineation. *International Journal of Imaging Systems and Technology* 6: 238-244. 1995.

Bibliography

1. Aguirre GK, Zarahn E, and D'Esposito M. Empirical Analyses of BOLD fMRI Statistics: II. Spatially Smoothed Data Collected under Null-Hypothesis Experimental Conditions. *Neuroimage* 5(3): 199-212. 1997.

2. Aguirre GK, Zarahn E, and D'Esposito M. The Variability of the Human, BOLD Hemodynamic Responses. *Neuroimage* 8(4), 360-369. 1998.
3. Ances BM, Zarahn E, and Detre JA. Non-Linearity of Either the Neutral-to-BOLD System or The Visual Stimulation-to-Neural System Demonstrated at 4.0 T. *Proc. Intl. Soc. Mag. Reson. Med.* 8. 2000.
4. Anderson AH, Danner DD, Friesen W, Avison RG, and Avison MJ. Direction and Analysis of Event-Related Responses in fMRI. *Proc. Intl. Soc. Mag. Reson. Med.* 6. 1998.
5. Bandettini PA, Jesmanowicz A, Wong EC, and Hyde JS. Processing Strategies for Time-Course Data Sets in Functional MRI of the Human Brain. *Magn. Reson. Med.* 30(2): 161-173. 1993.
6. Bandettini PA and Cox RW. Contrast in Single Trial fMRI: Interstimulus Interval Dependency with Blocked Strategies. *Proc. Intl. Soc. Mag. Reson. Med.* 6. 1998.
7. Bandettini PA and Cox RW. Event-Related fMRI Contrast When Using Constant Interstimulus Interval: Theory and Experiment. *Magn Reson Med* 43(4): 540-548. 2000.
8. Birn RM and Bandettini PA. Linearity of the BOLD Response to Varying Durations of Stimulus "OFF" Periods. *Proc. Intl. Soc. Mag. Reson. Med* 9. 2001.
9. Boynton GM, Engel SA, Glover GH, and Heeger DJ. Linear Systems Analysis of Functional Magnetic Resonance Imaging in Human V1. *J Neuroscience* 16(13): 4207-4221. 1996.
10. Bruder H, Fischer H, Reinfelder HE, and Schmitt F. Image Reconstruction for Echo Planar Imaging with Nonequidistant k-Space Sampling. *Magn. Reson. Med.* 23(2): 311-323. 1992.
11. Buckner RL. Event-Related fMRI and the Hemodynamic Response. *Hum Brain Map.* 6(5-6): 373-377. 1998.
12. Bullmore E, Brammer M, Williams SC, Rabe-Hesketh S, Janot N, David A, Mellers J, Howard R, and Sham P. Statistical Methods of Estimation and Interference for functional MR Image Analysis. *Magn. Reson. Med.* 35(2): 261-277. 1996.
13. Burock MA, Buckner RL, and Dale AM. Understanding Differential Responses in Event Related fMRI Through Linear Simulation. *Proc. Intl. Soc. Mag. Reson. Med.* 6. 1998.
14. Burock MA, Buckner RL, Woldorff MG, Rosen BR, and Dale AM. Randomized event-related experimental designs allow for extremely rapid presentation rates using functional MRI. *Neuroreport* 9: 3735-3739. 1998.
15. Buxton RB, Liu TT, and Wong EC. Nonlinearity of the Hemodynamic Response: Modeling the Neural and BOLD Contributions. *Proc. Intl. Soc. Mag. Reson. Med* 9. 2001.
16. Calhoun J, Adah T, Kraut M, and Pearlson G. A Weighted Least Squares Algorithm for Estimation and Visualization of Relative Latencies in Event-Related functional MRI. *Magn Reson Med.* 44(6): 947-54. 2000.
17. Carandini M, Heeger D, and Movshon J. 1997. Linearity and Normalization in Simple Cells of the Macaque Primary Visual Cortex. *J Neurosci* 17(21): 8621-8644.
18. Chen W and Ugurbil K. High spatial resolution functional magnetic resonance imaging at very-high magnetic field. *Topics in Magnetic Resonance Imaging.* 10(1): 63-78. 1999.
19. Dale AM. Optimal Experimental Design for Event-Related fMRI. *Hum. Brain Map.* 8(2-3): 109-114. 1999.
20. David O, Warnking J, and Segebarth C. Event-Related fMRI with pseudo-randomized inter-stimulus intervals (ISI). Optimization of the Distribution of the ISI. *Proc. Intl. Soc. Mag. Reson. Med.* 8. 2000.

21. D'Esposito M, Zarahn M, Aguirre GK, and Rypma B. The Effect of Normal Aging on the Coupling of Neural Activity to the BOLD Hemodynamic Response. *Neuroimage* 10(1): 6-14. 1999.
22. Feng C, Liu H, and Gao J. Coupling Between the Overshoots in BOLD Signal and Blood Flow Changes: A Computer Simulation Based on Balloon Model. *Proc. Intl. Soc. Mag. Reson. Med.* 9. 2001.
23. Forzane F, Riederer SJ, and Pelc, NJ. Analysis of T2 Limitations and Off-Resonance Effects on Spatial Resolution and Artifacts in Echo-Planar Imaging. *Magn. Reson. Med.* 14(1): 123-139. 1990.
24. Fransson P, Kruger G, Merboldt KD, and Frahm J. Temporal and Spatial MRI Responses to Subsecond Visual Activation. *Magnetic Resonance Imaging*, 17(1): 1-7. 1999.
25. Friston KJ, Jezzard P, and Turner R. Analysis of Functional MRI Time-Series. *Hum. Brain Map.* 1:153-171. 1994.
26. Friston KJ. Data Analysis: Basic Concepts and Overview. *SPM Short Course Notes*. Wellcome Department of Cognitive Neurology. 1997.
27. Glover GH. 3D z-shim Method for Reduction of Susceptibility Effects in BOLD fMRI. *Mag. Reson. in Med.* 42(2): 290-299. 1999.
28. Gopinath K, Briggs R, and Himes N. Examination of the Linearity of BOLD fMRI Responses in a Higher Level Cognitive System. *Proc. Intl. Soc. Mag. Reson. Med.* 9. 2001.
29. Grinvald A, Sloviter H, and Vanzetta I. Non-Invasive visualization of cortical columns by fMRI. *J Neurosci.* 3(2): 105-107. 2000.
30. Harel N, Shmuel A, Lee SP, K DS, Duong T, Yacoub E, and Hu X. Observation of Positive and Negative BOLD Signals in Visual Cortex. *Proc. Intl. Soc. Mag. Reson. Med.* 9. 2001.
31. Hathout GM, Gopi RK, Bandettini P, and Gambhir SS. The Lag of Cerebral Hemodynamics with Rapidly Alternating Periodic Stimulation: modeling for functional MRI. *Magnetic Resonance Imaging* 17(1): 9-20. 1999.
32. Heutzel S and McCarthy G. Evidence for a Refractory Period in the Hemodynamic Response to a Visual Stimuli as Measured by MRI. *Neuroimage* (5 pt1): 547-553. 2000.
33. Hoge RD, Atkinson J, Gill B, Crelier GR, Marrett S, and Pike GB. Non-Linear BOLD and Perfusion Dynamics in Human V1. *Proc. Intl. Soc. Mag. Reson. Med.* 7. 1999.
34. Hopfinger JB, Buchel C, Holmes AP, and Friston KJ. A Study of Analysis Parameters that Influence the Sensitivity of Event-Related fMRI Analyses. *Neuroimage* 11(4): 326-333. 2000.
35. Hutton C, Howseman AM, Josephs O, Friston K, and Turner R. The Effect of Inter-Stimulus Interval of Signal Response in fMRI. *Proc. Intl. Soc. Mag. Reson. Med.* 6. 1998.
36. Janz C, Heinrich S, Kornmayer J, Bach M, and Hennig J. Combination of fMRI and VEP Recording: The BOLD Response is not a Linear Transform of the Average Neuronal Activity. *Proc. Intl. Soc. Mag. Reson. Med.* 9. 2001.
37. Janz C, Kornmayer J, and Hennig J. Investigation of Linear vs. Non-Linear BOLD Effects in the Transition from Single Event to Continuous Stimulation. *Proc. Intl. Soc. Mag. Reson. Med.* 7. 1999.
38. Janz C, Speck O, and Hennig J. Time-Resolved Measurements of Brain Activation After short Visual Stimulus: New Results on the Physiological Mechanisms of the Cortical Response. *NMR in Biomedicine* 10(4-5), 222-229. 1997.

39. Jezzard P and Turner R. Magnetic Resonance Imaging Methods for Study of Human Brain Function and their Application at High Magnetic Field. *Computerized Medical Imaging and Graphics* 20(6): 467-81. 1996.
40. Jezzard P. Intrinsic Magnetic Field Distortions Caused by Head Motion in Functional MRI Data Sets. *Proc. Intl. Soc. Mag. Reson. Med.* 7. 1999.
41. Josephs O, Turner R, and Friston KJ. Event-Related fMRI. *Proc. Intl. Soc. Mag. Reson. Med.* 6. 1998.
42. Kershaw J, Abe S, Kashikura K, Zhang X, and Kanno I. Bayesian Inference for the Shape of the Hemodynamic Response Function in Event-Related fMRI. *Proc. Intl. Soc. Mag. Reson. Med.* 8. 2000.
43. Kim SG and Ugurbil K. Comparison of Blood Oxygenation and Cerebral Blood Flow Effects in fMRI: estimation of relative oxygen consumption change. *Mag. Reson. Med.* 38(1): 59-65. 1997.
44. Kim SG and Ugurbil K. Functional Magnetic Resonance Imaging of the Human Brain. *J Neurosci.* 74: 229-43. 1997.
45. Kruggel F, Wiggins CJ, Herrmann CS, and von Cramon DY. Recording of the Event-Related Potentials during functional MRI at 3.0 Tesla field strength. *Mag. Reson. Med.* 44(2): 277-282. 2000.
46. Kruggel F and von Cramon DY. Temporal Properties of the Hemodynamic Response in Functional MRI. *Hum. Brain Map.* 8(4): 259-271. 1999.
47. Kruger G, Fransson P, Merboldt KD, and Frahm J. Does Stimulus Quality affect the Physiologic MRI Responses to Brief Visual Activation? *Neuroreport* 10(6): 1227-1281. 1999.
48. Kruger G, Kastrup A, Takahashi A, and Glover GH. Simultaneous Monitoring of Dynamic Changes in Cerebral Blood Flow and Oxygenation during Sustained Activation of the Human Visual Cortex. *Neuroreport* 1999 September 29; 10(14): 2939-2943.
49. Kushnir T, Grill-Spector K, Mukamel R, Malach R, and Itzchak Y. Linear Aspects of the BOLD Response in Object Related Visual Areas: An fMRI study. *Proc. Intl. Soc. Mag. Reson. Med.* 7. 1999.
50. Lee SL, Wang P, Ogawa S, and Kim SG. Quantitative Relationship between BOLD signals and neural activity. *Proc. Intl. Soc. Mag. Reson. Med.* 9. 2001.
51. Li TQ, Haefelin TN, Chan B, Kastrup A, Jonsson T, Glover GH, and Mossey ME. Assessment of Hemodynamic Response during Focal Neural Activity using Bolus Tracking, Arterial Spin Labeling and BOLD Techniques. *Neuroimage* 12(4): 442-451. 2000.
52. Liu HL and Gao JH. Perfusion-based Event-Related functional MRI. *Mag. Reson. Med.* 42(6): 1011-1013. 1999.
53. Marchini JL and Ripley BD. A New Statistical Approach to Detecting Significant Activation in Functional MRI. *Neuroimage* 12 (4): 366-380. 2000.
54. Menon RS and Kim SG. Spatial and Temporal Limits in Cognitive Neuroimaging with fMRI. *Trends in Cognitive Sciences.* 3(6): 207-216. 1999.
55. Menon RS, Gati JS, Goodyear BG, Luknowsky DC, and Thomas CG. Spatial and Temporal Resolution of functional Magnetic Resonance Imaging. *Biochemistry and Cell Biology* 76(2-3): 560-571. 1998.
56. Menon RS, Thomas CG, and Gati JS. Investigation of BOLD contrast in fMRI using multi-shot EPI. *NMR in Biomedicine* 10(4-5): 179-182. 1997.

57. Miezin FM, Maccotta L, Ollinger JM, Peterson SE, and Buckner RL. Characterizing the Hemodynamic Response: Effects of Presentation Rate, Sampling Procedure, and the Possibility of Ordering Brain Activity Based on Relative Timing. *Neuroimage* 11(6 Pt 1): 735-759. 2000.
58. Miller KL, Luh WM, Liu TT, Martinez A, Obata T, Wong EC, Frank LR, and Buxton RB. Nonlinear Temporal Dynamics of the Cerebral Blood Flow Response. *Hum Brain Map* 13(1): 1-12. 2001.
59. Ogawa S, Menon RS, Kim SG, and Ugurbil K. On the Characteristics of functional Magnetic Resonance Imaging of the Brain. *Annual review of biophysics and biomolecular structure*. 27: 447-474. 1998.
60. Ogawa S, Tank DW, Menon R, Ellerman JM, Kim SG, Merkle H, and Ugurbil K. Intrinsic Signal Changes Accompanying Sensory Stimulation: Functional brain mapping with magnetic resonance imaging. *Proc. Natl. Acad. Sci. USA*. 89(13): 5951-5955. 1992.
61. Ogawa S, Lee TM, Stepnoski R, Chen W, Zhu XH, and Ugurbil K. An Approach to Probe some Neural Systems Interaction by functional MRI at Neural Time Scale Down to Milliseconds. *Proc. Natl. Acad. Sci.* 97(20): 11026-11031. 2000.
62. Ollinger JM, Shulman GL, and Corbetta M. Separating processes within a trial in event-related functional MRI. *Neuroimage* 13(1): 210-217. 2001.
63. Pfeuffer J, van de Moortele PF, Adrainy G, Hu X, and Ugurbil K. Sub-Millimeter Event-Related fMRI at High Temporal Resolution. *Proc. Intl. Soc. Mag. Reson. Med.* 9. 2001.
64. Pfeuffer J, van de Moortele PF, Yacoub E, Adrainy G, Shmuel A, Anderson P, Merkle H, Ugurbil K, and Hu X. Single-Shot Imaging at Sub-Millimeter Resolution Using Adiabatic Outer-Volume-Suppression. *Proc. Intl. Soc. Mag. Reson. Med.* 9. 2001.
65. Pfeuffer J, Tkac I, Provencher SW, and Gruetter R. Toward an in vivo Neurochemical Profile: quantification of 18 metabolites in short-echo-time (1)H NMR spectra of the rat brain. *J Magn Reson.* 141(1): 104-120. 1999.
66. Raichle M. Behind the Scenes of functional Brain Imaging: A historical and physiological perspective. *Proc. Natl. Acad. Sci. USA*. 95(3): 765-772. 1998.
67. Rajapakse J, Kruggel F, Maisog JM, and von Cramon DY. Modeling Hemodynamic Response for Analysis of Functional MRI Time-Series. *Hum Brain Map* 6(4): 283-300. 1998.
68. Rees G, Howseman A, Josephs O, Frith CD, Friston KJ, and Frackowiak RS. Characterizing the Relationship between BOLD Contrast and Regional Cerebral Blood Flow Measurements by Varying the Stimulus Presentation Rate. *Neuroimage* 6(4): 270-278. 1997.
69. Richter W. High Temporal Resolution functional Magnetic Resonance Imaging at very-high-field. *Topics in Magnetic Resonance Imaging* 10(1): 51-62. 1999.
70. Rosen BR, Buckner RL, and Dale AM. Event-Related functional MRI: Past, present, and future. *Proc. Natl. Acad. Sci. USA*. 95(3): 773-780. 1998.
71. Shmuel A, Yacoub E, Pfeuffer J, van de Moortele PF, Adrainy G, Ugurbil K, and Hu X. Reproducibility of BOLD Response in the Human Brain as Measured at High-Resolution at 7 Tesla. *Proc. Intl. Soc. Mag. Reson. Med.* 8. 2000.
72. Turner R, Howseman A, Rees GE, Josephs O, and Friston K. Functional Magnetic Resonance Imaging of the Human Brain: data acquisition and analysis. *Experimental Brain Research* 123(1-2): 5-12. 1998.
73. Ugurbil K, Hu X, Chen W, Zhu XH, Kim SG, and Georgopoulos A. Functional Mapping in the Human Brain using High Magnetic Fields. *Phil. Trans. R. Soc. Lond. B.* 354(1387): 1195-1213. 1999.

74. Vazquez A and Noll D. Physiological Modeling of BOLD Hemodynamics. *Proc. Intl. Soc. Mag. Reson. Med.* 8. 2000.
75. Villringer A and Dirnagl U. Coupling of Brain Activity and Cerebral Blood Flow: Basis of functional neuroimaging. *Cerebrovasc Brain Metab Rev.* 7:240-276. 1995.
76. Yacoub E, Shmuel A, Pfeuffer J, van de Moortele PF, Adriany G, Ugurbil K, and Hu X. Dynamics of the BOLD Response at Ultrahigh fields Revealed at High Spatial and Temporal Resolutions. *Proc. Intl. Soc. Mag. Reson. Med.* 9. 2001.
77. Yang Y, Engelien A, Engelien W, Xu S, Siberseig, A, and Stern E. A Hemodynamic-Response Based Sequence for Event-Related fMRI Studies without Interference of Scanner Noise. *Proc. Intl. Soc. Mag. Reson. Med.* 7. 1999.
78. Yang Y, Engelien W, Pan H, Xu S, Stern E, and Silbersweig DA. Assessment of linearity of Perfusion and BOLD Response Functions in Event-Related Functional MRI. *Proc. Intl. Soc. Mag. Reson. Med.* 8. 2000.
79. Yang Y, Wen H, Mattay VS, Balaban RS, Frank JA, and Duyn JH. Comparison of 3D BOLD functional MRI with Spiral Acquisition at 1.5 and 4.0 T. *Neuroimage* 9(4): 446-451. 1999.
80. Zarahn E, Aguirre GK, and D'Esposito M. A Trial-Based Experimental Design for fMRI. *Neuroimage* 6(2): 122-138. 1997.
81. Zarahn E. Testing for Neural Responses During Temporal Components of Trials with BOLD fMRI. *Neuroimage.* 11(6 Pt 1): 783-96. 2000.
82. Zarahn E, Aguirre GK, and D'Esposito M. Empirical Analyses of BOLD fMRI Statistics: I. Spatially Unsmoothed Data Collected under Null-Hypothesis Conditions. *Neuroimage* 5(3): 179-197. 1997.